
STATISTICAL INFERENCE OF MINIMALLY COMPLEX MODELS

A PREPRINT

Clélia de Mulatier

Institute for Theoretical Physics and Informatics Institute
University of Amsterdam, Amsterdam, the Netherlands
Department of Physics and Astronomy
University of Pennsylvania, Philadelphia, USA
c.m.c.demulatier@uva.nl

Paolo P. Mazza

Institute for Theoretical Physics
University of Tübingen
Auf der Morgenstelle 14, 72076 Tübingen, Germany
paolopietro.mazza@gmail.com

Matteo Marsili

The Abdus Salam International Centre for Theoretical Physics (ICTP)
Strada Costiera 11, I-34014 Trieste, Italy
marsili@ictp.it

September 2021

ABSTRACT

Finding the model that best describes a high dimensional dataset is a daunting task. For binary data, we show that this becomes feasible when restricting the search to a family of *simple* models, that we call Minimally Complex Models (MCMs). These are spin models, with interactions of arbitrary order, that are composed of independent components of minimal complexity (Beretta et al., 2018). They tend to be *simple* in information theoretic terms, which means that they are well-fitted to specific types of data, and are therefore easy to falsify. We show that Bayesian model selection restricted to these models is computationally feasible and has many other advantages. First, their evidence, which trades off goodness-of-fit against model complexity, can be computed easily without any parameter fitting. This allows selecting the best MCM among all, even though the number of models is astronomically large. Furthermore, MCMs can be inferred and sampled from without any computational effort. Finally, model selection among MCMs is invariant with respect to changes in the representation of the data. MCMs portray the structure of dependencies among variables in a simple way, as illustrated in several examples, and thus provide robust predictions on dependencies in the data. MCMs contain interactions of any order between variables, and thus may reveal the presence of interactions of order higher than pairwise.

Keywords Statistical inference · Spin models · Information theory

Significance statement. Finding the model that best captures patterns hidden within noisy data is fundamental for science but challenging. Here we propose a novel approach for extracting the simplest explanation from binary data. To do so we introduce a new family of models called Minimally Complex Models (MCMs). In these models, variables are connected with interactions of arbitrary order that can identify any patterns of data. Yet, MCMs are simple in information theoretic terms, and provide robust predictions on dependencies between variables, that are easy to falsify. Our approach contrasts with usual methods by focusing on simple representation of data, opening new avenues of research in statistical inference of high dimensional data.

1 Introduction

“All models are wrong, but some models are useful” [1]. This statement is particularly appropriate in the context of statistical inference of high dimensional data. Recent spectacular advances in machine learning have shown that very complex models, such as deep neural networks [2], can be very “useful” in learning hidden features in high dimensional

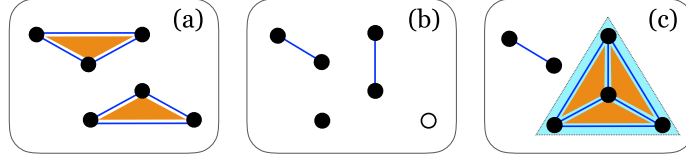


Figure 1: (colors online) **Examples of Minimally Complex Models** for a 6-spin system. Models are represented by diagrams: single spin variables are dots, full in presence of a local field, empty otherwise; pairwise interactions are blue lines; 3-spin interactions are orange triangles; and 4-spin interactions are light blue polygons including four spins. Note that all three models are displayed in a special basis.

data, making it possible to generalize from examples. Models that encode the Laws of Nature, refer to a different notion of “usefulness”. As argued by Wigner [3], they describe regularities – such as how bodies fall under the effect of gravity – in *simple* forms involving only few variables and parameters. These regularities occur in ways that are independent of many conditions that could affect them. Simple models, such as Newton’s law, tell us more about independence than about dependence. Their simplicity reflects specific principles – such as invariances, symmetries and conservation laws – that are easy to falsify. In this paper, we are interested in performing statistical inference for binary data with models that display similar simplicity.

In information theory, the *simplicity* of a statistical model is defined unambiguously in terms of the Minimum Description Length (MDL) complexity, which is the minimal number of bits required to encode the model [4]. This complexity is a measure of the number of different datasets that can be described by the same parametric model [5], and therefore, of the flexibility of the model in fitting broad types of data. A *simple* model thus fits well few types of data and, as a consequence, is easy to falsify. In Bayesian inference, the MDL complexity predicts how much a model would be penalised due to its flexibility to data. In the context of binary data, Beretta *et al.* [6] have studied the MDL complexity of spin models, which are maximum entropy models with interactions of arbitrary order¹. They argue that, with the same number of parameters, the simplest models are those for which statistical dependencies concentrates on the smallest subset of variables. By contrast, pairwise spin models – which have been used to model a variety of systems from neuronal activity [7, 8] to voting outcomes [9] – turn out to be very complex. Interestingly, the simplest spin models are also very easy to infer [6], while statistical inference of pairwise spin models is known to be computationally challenging [10, 11, 12, 13, 14].

In this paper, we show that this latter property of the simplest spin models make Bayesian Model Selection (BMS) possible within a remarkably broad family of simple models for binary data (for which maximum likelihood and model evidence are easy to compute). These models, which we call *Minimally Complex Models* (MCMs), are spin models formed of independent components of minimal complexity. In some representations an MCM corresponds to a partition of the variables in independent parts (or “communities”), with no interactions between the parts and with all possible interactions within each part (see Fig. 1). The best MCM for a given dataset thus captures a global structure of dependencies and independencies in the data, providing robust predictions on dependencies between variables. Besides being simple and easy to infer, MCMs also enjoy properties that make statistical inference invariant under changes in the representation of data. Finally, inferred MCMs can also be sampled from with minimal computational effort.

In what follows, we formally define MCMs and discuss how to compare them in the context of BMS. As the set of potential MCMs to compare is still huge (see Fig. 2), we then propose different heuristics to find the best MCMs for data. Our results are finally illustrated on several test cases, where one can appreciate how our approach uncovers global data structures of dependencies that are consistent with the discussed phenomena.

Bayesian Model Selection of Spin Models

A binary dataset $\hat{\mathbf{s}} = (\mathbf{s}^{(1)}, \dots, \mathbf{s}^{(N)})$ is a set of N independent observations of spin configurations $\mathbf{s} = (s_1, \dots, s_n)$, where $s_i = \pm 1$. In the following, we assume that each configuration $\mathbf{s}^{(i)}$ is independently drawn from an unknown distribution, which we aim to infer. To do so, we consider the following parametric family of probability distributions:

$$p(\mathbf{s} | \mathbf{g}, \mathcal{M}) = \frac{1}{Z_{\mathcal{M}}(\mathbf{g})} \exp \left(\sum_{\mu \in \mathcal{M}} g^{\mu} \phi^{\mu}(\mathbf{s}) \right), \quad (1)$$

¹Spin models include the so-called Ising model as a special case, when only pairwise interactions are considered.

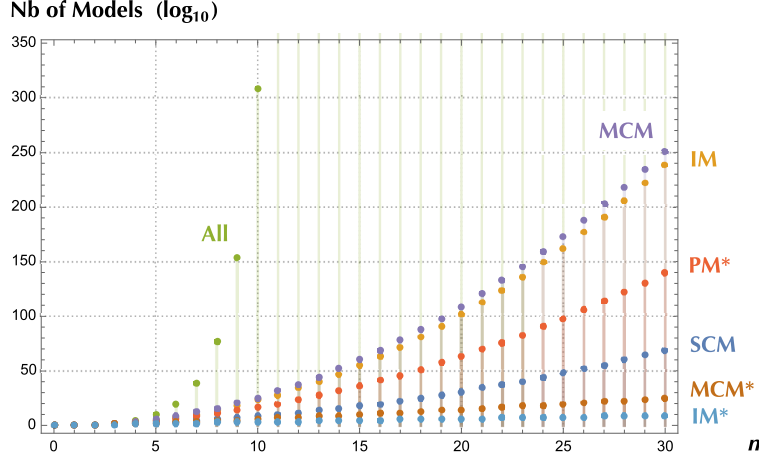


Figure 2: (colors online) **Number of spin models** as a function of the system size n for different families (see SI Sec. S2 for details on enumerations): all spin models (green), all Minimally Complex Models (MCMs, violet), all Independent Models (IM, orange), and all models with a Single Complete Component (SCM, dark blue). MCM* and IM* indicate respectively the number of MCM and IM that share the same preferred basis. For comparison, we also reported the number of Pairwise Models (PM*). The number of IMs and of MCMs both grow exponentially with n , roughly as 2^{n^2} , whereas the number of PM* grows as $2^{n^2/2}$. The number of MCM* grows slower than n^n . Note that the y -axis reports the logarithm base 10 of the number of models. For example at $n = 9$, there are of the order of 10^{153} models, but only 10^{20} MCMs, which include 10^{18} IM and 10^5 MCM*; there are 10^{13} PM*.

where $\mathcal{M} = \{\mu_1, \dots, \mu_K\}$ is a set of K interactions of arbitrary order, and the μ_i 's are binary vectors encoding which spins are involved in each interaction. Any choice of the set \mathcal{M} of interactions defines a spin model. The operators² $\phi^\mu(\mathbf{s}) = \prod_{i \in \mu} s_i$ are the product spin operators associated to the interactions μ of \mathcal{M} , while the conjugate parameters g^μ modulate the strength of the interactions. For example, pairwise spin models contain interactions $\phi^\mu(\mathbf{s}) = s_i s_j$ between pairs of spins. Finally, the partition function $Z_{\mathcal{M}}(\mathbf{g})$ ensures normalisation (see SI Sec. 1 for more details on spin models).

Equation (1) defines a complete family of models, capable of describing all possible patterns of binary data with an appropriate choice of the set \mathcal{M} of operators [15]. In absence of prior knowledge on the system, one must ideally compare the performance of all spin models to find which one best describes a dataset $\hat{\mathbf{s}}$. In the Bayesian approach, the best model \mathcal{M} is the one achieving the largest posterior probability $P(\mathcal{M} | \hat{\mathbf{s}})$, which is obtained with Bayes' theorem after computing the *evidence* [16]:

$$P(\hat{\mathbf{s}} | \mathcal{M}) = \int_{\mathbb{R}^M} d\mathbf{g} \prod_{i=1}^N p(\mathbf{s}^{(i)} | \mathbf{g}, \mathcal{M}) p_0(\mathbf{g} | \mathcal{M}), \quad (2)$$

where $p_0(\mathbf{g} | \mathcal{M})$ is a prior distribution over the parameters. We assume a uniform prior over the models \mathcal{M} , such that the best model for data is also the one that maximizes the evidence. Furthermore, we assume that $p_0(\mathbf{g} | \mathcal{M})$ takes the form of Jeffreys' prior [17]. With this choice, it has been shown [5] that in the limit of large datasets ($N \rightarrow \infty$) the model \mathcal{M} maximizing the evidence in Eq. (2) is also the one providing the most succinct description of the data in the Minimum Description Length (MDL) principle [18, 19, 4]. Indeed, in the large N limit, one finds [5] that:

$$\log P(\hat{\mathbf{s}} | \mathcal{M}) \underset{N \rightarrow \infty}{\simeq} \log P(\hat{\mathbf{s}} | \hat{\mathbf{g}}, \mathcal{M}) - \frac{K}{2} \log \left(\frac{N}{2\pi} \right) - c_{\mathcal{M}}, \quad (3)$$

where $\hat{\mathbf{g}}$ are the maximum likelihood parameters, and $c_{\mathcal{M}}$ is the geometric complexity of model \mathcal{M} . The second term is a first order model complexity which is proportional to the number K of interactions in the model. The sum of these two complexity terms is the MDL complexity.

Yet, computing the evidence in Eq. (2) or the complexity $c_{\mathcal{M}}$ for a generic spin model \mathcal{M} is computationally challenging [6]. In addition, the number of potential models to compare is huge – in an n -spin system, there exists $2^n - 1$ interactions of arbitrary order, and therefore $2^{2^n - 1}$ potential models –, making the exhaustive search among all spin

²The product is over all index i such that the i -th element of the binary vector μ is 1.

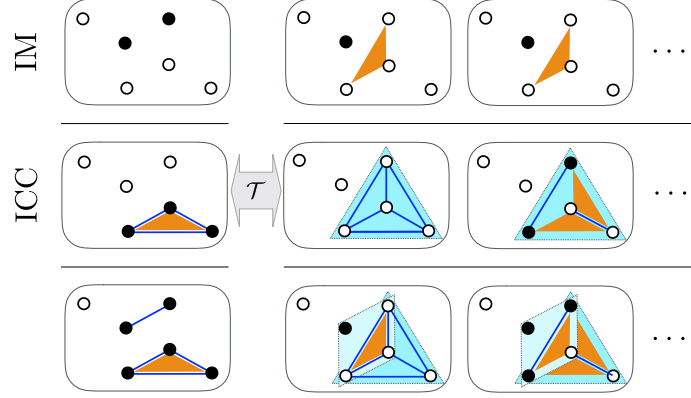


Figure 3: (colors online) **Examples of MCMs and gauge transformations.** Models are represented with the same notations as in Fig. 1. All the models are MCMs. In the first column, the first model is an independent model (IM) composed of two independent operators, the second is a model composed of a single independent complete component (ICC), and the last one is a MCM composed of two ICCs. In each column, models of each row are obtained by the same gauge transformation \mathcal{T} of these models, and therefore have the same properties than the original model (i.e., they are respectively, IM, MCM with one ICC, and MCM with two ICCs).

models unfeasible, even for small systems (see Fig. 2). A possible solution to this hurdle is to restrict model selection to a smaller family of models, such as pairwise models. For this family, model selection turns into a problem of graph reconstruction [10, 12], that aims at identifying the network of interactions among spins. A plethora of methods and results have been derived within this framework [11, 14, 13]. Here, we propose to focus on a different family of models, the *minimally complex models* (MCMs).

Minimally Complex Models (MCMs)

Definition

MCMs are a subset of the spin models defined in Eq. (1), for which the set \mathcal{M} of interactions is the union of *independent complete components* (ICCs) \mathcal{M}_a :

$$\mathcal{M} = \bigcup_{a \in \mathcal{A}} \mathcal{M}_a. \quad (4)$$

A *complete component* is a set \mathcal{M}_a of interactions verifying that, for any two $\mu, \nu \in \mathcal{M}_a$, the interaction $\mu \oplus \nu$ associated with the spin operator $\phi^{\mu \oplus \nu}(\mathbf{s}) \doteq \phi^\mu(\mathbf{s}) \phi^\nu(\mathbf{s})$ also belongs to \mathcal{M}_a . Furthermore, complete components are said *independent* if they do not overlap. Therefore, in Eq. (4), for any two distinct $(a, a') \in \mathcal{A}$, $\mathcal{M}_a \cap \mathcal{M}_{a'} = \emptyset$. Figure 3 shows several examples of MCMs.

Preferred basis of an MCM

A *basis* \mathbf{b} of a model \mathcal{M} is a minimal set of r independent operators, $\mathbf{b} = (\phi_1, \dots, \phi_r)$, that can generate all the operators of \mathcal{M} , i.e., any operators $\phi \in \mathcal{M}$ can be written as a unique product of elements of \mathbf{b} . The cardinal r of such basis is called the *rank* of \mathcal{M} (necessarily $r \leq n$). We recall that a set \mathbf{b} of operators is said *independent* if none of its operators can be obtained as a product of other operators of \mathbf{b} [6]. For example, $\mathbf{b} = \{s_1, s_2, s_3\}$ and $\mathbf{b}' = \{s_1, s_1 s_2, s_1 s_2 s_3\}$ are two sets of independent operators, and both sets are possible bases for the model $\mathcal{M} = \{s_1, s_2, s_1 s_2, s_3\}$.

By definition, a *complete component* \mathcal{M}_a is a special case of model that contains all the $2^{r_a} - 1$ operators generated by its basis $\mathbf{b}_a = (\phi_1, \dots, \phi_{r_a})$. As a direct consequence, the number of operators of an MCM is

$$K = \sum_{a \in \mathcal{A}} (2^{r_a} - 1). \quad (5)$$

Note that the choice of the basis of an ICC is not unique. For example, \mathbf{b} and \mathbf{b}' both generate the same ICC, and are therefore two possible bases for that ICC.

Finally, as a result of the *independence* between the complete component \mathcal{M}_a of an MCM \mathcal{M} , the union of chosen bases \mathbf{b}_a for each \mathcal{M}_a forms a basis \mathbf{b} of \mathcal{M} ,

$$\mathbf{b} = \cup_{a \in \mathcal{A}} \mathbf{b}_a. \quad (6)$$

In this basis, \mathcal{M} exactly corresponds to a partition of the basis variables into ICCs (see examples in Fig. 1, and in the first column of Fig. 3). We refer to such basis as a *preferred* basis of an MCM. A direct implication of Eq. (6) is that the rank of an MCM is $r = \sum_{a \in \mathcal{A}} r_a$.

Properties

Let us now discuss properties of MCMs. We first observe that, as a consequence of Eq. (6), the state probability distribution of an MCM \mathcal{M} factorizes over the probability distribution of its ICCs, when expressed in terms of the operators $\mathbf{b}(\mathbf{s}) = \cup_a \mathbf{b}_a(\mathbf{s})$ of a preferred basis of \mathcal{M} :

$$p(\mathbf{s} | \mathbf{g}, \mathcal{M}) = \frac{1}{2^{n-r}} \prod_{a \in \mathcal{A}} p_a(\mathbf{b}_a(\mathbf{s}) | \mathbf{g}_a, \mathcal{M}_a). \quad (7)$$

The prefactor corresponds to a $1/2$ probability for each of the $(n-r)$ spin variables not modeled by \mathcal{M} (see for instance the spins represented by empty dots in the MCMs of the first column of Fig. 3). Note that each p_a is a probability distribution over r_a spin variables. Importantly, Eq. (7) implies that the evidence of an MCM factorizes over its ICCs. In addition, the evidence of each ICC is remarkably simple to compute (see Methods 1.1), leading to the following expression for the evidence of an MCM \mathcal{M} for any dataset $\hat{\mathbf{s}}$:

$$P(\hat{\mathbf{s}} | \mathcal{M}) = \frac{1}{2^{N(n-r)}} \prod_{a \in \mathcal{A}} \frac{\Gamma(2^{r_a-1})}{\Gamma(N + 2^{r_a-1})} \prod_{\mathbf{b}_a} \frac{\Gamma(k_{\mathbf{b}_a} + \frac{1}{2})}{\sqrt{\pi}}, \quad (8)$$

where Γ is the gamma function, N is the number of datapoints in $\hat{\mathbf{s}}$, and $k_{\mathbf{b}_a}$ is the number of times that the basis operators take the value \mathbf{b}_a over the dataset. The maximum likelihood distribution also takes a simple form (see Methods 1.1):

$$P(\hat{\mathbf{s}} | \hat{\mathbf{g}}, \mathcal{M}) = \frac{1}{2^{N(n-r)}} \prod_{a \in \mathcal{A}} \prod_{\mathbf{b}_a} \left(\frac{k_{\mathbf{b}_a}}{N} \right)^{k_{\mathbf{b}_a}}. \quad (9)$$

This makes sampling from the maximum likelihood distribution a very easy task (see Methods 1.3).

Another important property is that the family of MCMs is invariant under the *gauge transformations* (GTs) defined in Ref. [6]. A GT \mathcal{T} is a bijection of the set of states into itself (automorphisms), where a new state \mathbf{s}' is defined as a function of the original state \mathbf{s} by a set of n independent operators: $\mathbf{s}' = \mathcal{T}(\mathbf{s}) = (\phi_1(\mathbf{s}), \dots, \phi_n(\mathbf{s}))$. Such transformations are also bijections of the set of all operators into itself³, and therefore of the set of models into itself⁴. Notice that the order of an operator, i.e. the number of spins that occur in it, is not invariant under GTs (see Fig. 3 for examples of GTs). However, the mutual relation between the operators of a model is preserved under a GT⁵ [6], i.e., if ϕ_1 and ϕ_2 are two operators and $\phi_{1+2} = \phi_1\phi_2$, then the gauge transformed operator ϕ'_{1+2} is still the product of the transformed operators ϕ'_1 and ϕ'_2 . In particular, under a GT an ICC maps into an ICC with same rank, and an IM maps into an IM with same rank. And as a consequence, applying a GT to an MCM returns an MCM with the same number ICCs and same rank sequence (see Fig. 3). On the contrary, the family of pairwise models is not invariant under GTs. In BMS, invariance under GTs of the considered family of models ensures that the outcome of the inference process is independent of the *gauge* in which the data is expressed.

Finally, Ref. [6] shows that, among all models with the same number of parameters, ICCs are the models with the lowest MDL complexity. As MCMs are formed by the union of *independent* ICCs, their MDL complexity is the sum of the complexity of each ICC, and is thus expected to be small. We conjecture that MCMs are the models with the lowest MDL complexity among all spin models with the same number of parameters and the same rank. We verified that this is true for all models with up to 4 spin variables (see Fig. S1). Although this statement has yet to be proven in the general case, our belief in its likely correctness motivated our choice of the name *minimally complex models*.

³A transformed operator ϕ' is obtained from the original operator ϕ by $\phi'(\mathbf{s}') = \phi(\mathcal{T}^{-1}(\mathbf{s}'))$.

⁴A transformed model $\mathcal{M}' = \mathcal{T}(\mathcal{M})$ is obtained by transforming each operator of the original model \mathcal{M} .

⁵This mutual relation between operators of a model is called the loop structure of the model in Ref. [6]. Models with the same loop structure have the same Fisher information matrix.

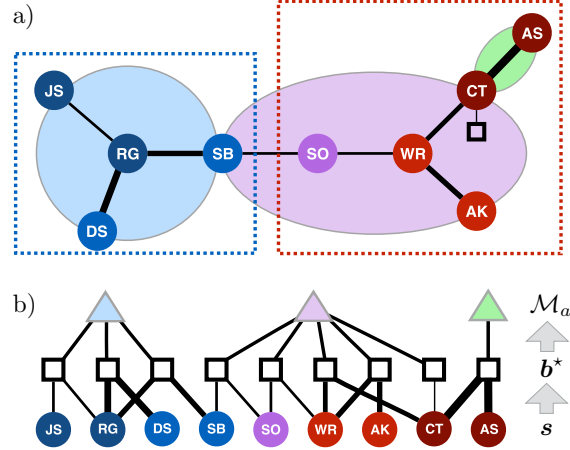


Figure 4: **Analysis of the US Supreme Court Data.** Justices are represented by circles labelled by their initials: Ruth Bader Ginsburg (RG), John P. Stevens (JS), David Souter (DS), Stephen Breyer (SB), Sandra Day O’Connor (SO), William Rehnquist (WR), Anthony Kennedy (AK), Clarence Thomas (CT), Antonin Scalia (AS). Colours represent their political orientation taken from Ref. [9]. **a) The best MCM, represented in the original basis of variables** (i.e., the justices’ votes). The best IM is composed of 8 pairwise interactions, represented by links between the nodes with width proportional to their strength, and 1 single body interaction represented by a square on CT. The strongest interaction has $\langle s_{CT}s_{WR} \rangle \simeq 0.86$, whereas the weakest has $\langle s_{CT} \rangle \simeq -0.45$. The three shaded circles indicate the overall best MCM, which was computed in the basis of these interactions. The red and blue dotted squares indicate the best MCM based on the original basis of spin variables (i.e., for which $\mathbf{b} = \mathbf{s}$). **b) Factor graph representation of the best MCM.** Spin variables \mathbf{s} are represented by circles. The inference procedure first identifies the best basis \mathbf{b}^* of independent operators, denoted by squares, and then the best clustering of these operators into ICCs \mathcal{M}_a , denoted by triangles. Each square in the second layer corresponds to one of the basis interactions represented in Fig. a.

Bayesian Model Selection

All together, these properties are good reasons for restricting BMS to the set of MCMs. First, Eq. (7) shows that finding the best MCM provides sharp predictions on independencies between variables of different ICCs. Second, the fact that the computation of the evidence in Eq. (8) is straightforward from the data greatly simplifies the task of BMS, and comparison between models can be done without inferring any parameter and directly on the basis of their evidence. Finally, invariance under GTs ensures that the selected models are independent of the ways in which data is represented.

Yet the number of MCMs is still huge, even for moderate values of n (growing roughly as 2^{n^2} , see Fig. 2). To find the MCM with maximal evidence, we propose to divide the search in two steps. First, we look for the best model among all *Independent Models* (IM), which are MCMs with $r_a = 1$ for all $a \in \mathcal{A}$ (see examples in Fig. 3). The maximization of the evidence over this family can be done by finding the set \mathbf{b}^* of the n most biased independent operators in the dataset (see Methods 1.2). Although the number of IMs is also huge ($\sim 2^{n^2}$), finding the best IM with this procedure only takes of the order of $n 2^n$ operations. Once the best IM \mathbf{b}^* is singled out, we reduce our search for the best MCM to the subset of models that admit \mathbf{b}^* as a preferred basis. This entails partitioning the vector \mathbf{b}^* into ICCs, and finding which such partition maximizes the evidence. The outcome of this algorithm can be represented as a factor graph with three layers (see Fig. 4b), one connecting the original variables \mathbf{s} with the basis vector \mathbf{b}^* , and the other connecting the latter to the ICCs \mathcal{M}_a . A program implementing this algorithm has been made available by the author at Ref. [20]. Note that the number of IMs is not much smaller than the number of MCMs, whereas the number of MCMs with the same basis (denoted as MCM* in Fig. 2) is much smaller. Indeed, the number of such models is given by the Bell number of n , which grows slower than $(n/\log(n))^n$ [21]. This makes exhaustive search possible for moderate system sizes ($n \lesssim 15$). Larger systems require further heuristics that will be discussed below.

MCM selection for small systems

Voting data from the US Supreme Court [9]

Let us first illustrate our method with the analysis of voting data from the US Supreme Court database [22]. The dataset we consider is composed of the votes of the $n = 9$ justices on $N = 895$ cases debated during the second Rehnquist

Court. As in Ref. [9], voting outcomes were re-labeled using the political inclination (if known) of each debated case, such that, for each case, each judge casts a vote $s_i = +1$ if the decision is conservative-oriented, or $s_i = -1$ if it is liberal-oriented. Ref. [9] showed that a fully connected pairwise model is able to explain higher order features of the data. Ref. [23] further analysed the data within a more general scheme, showing that pairwise interactions are indeed prevalent in this dataset. The size of the system ($n = 9$) is sufficiently small to perform the exhaustive search described in the previous section⁶.

The best IM is displayed in Fig. 4.a and has a very large log-evidence ($\log E = -3327$) compared to the usual IM composed of 9 single spin operators (i.e., the IM based in the original basis of the data $\mathbf{b} = \mathbf{s}$, for which $\log E = -5258$). Interestingly, we found that the 9 most biased independent operators of the data are all single- or two-body, although the selection procedure takes into account interactions of all orders. This confirms the prevalence of low order interactions in the system. Moreover, these 9 interactions alone account for more than 80% of the information captured by the fully connected pairwise model with 45 interactions, and therefore they provide a meaningful representation of the data. With the exception of the single spin interaction on CT, all these interactions are pairwise. They connect justices with similar political orientation [9] and define a network that spans the entire political spectrum. Interestingly, the strength of the interactions increases towards the extremes of the political spectrum and is weaker at the center. Without the single spin interaction, which is much weaker than the other interactions, the systems would be invariant under spin reversal ($s_i \rightarrow -s_i$). The single spin interaction on CT introduces a bias towards conservative votes.

The best MCM can be found from the best IM by using algorithms for generating all possible partitions of a set [24, 25, 26]. There are 115975 different MCMs that can be generated from a given IM with $n = 9$. For the US Supreme court data, the best MCM is composed of three ICCs (see Fig. 4). The first consists solely of the interaction between AS and CT, suggesting that AS's voting patterns conditioned on that of CT is mostly independent of all the others. The second ICC groups the three interactions between judges on the liberal side of the political spectrum, suggesting that, conditioned on the vote of SB, the voting patterns of RG, JS and DS is mostly independent of the votes of the other judges. Finally, the third ICC groups interactions on the conservative-center side of the political spectrum. For comparison, Fig. 4.a also shows the best MCM whose preferred basis is the original basis of the data (i.e., with $\mathbf{b} = \mathbf{s}$). This MCM divides the court into two independent components that happen to match with the justices' political orientations. Yet the evidence of this model ($\log P(\hat{s}|\mathcal{M}) = -3156.71$) is considerably smaller than that of the MCM build from the best IM \mathbf{b}^* ($\log P(\hat{s}|\mathcal{M}) = -3300.97$). The evidence of the best MCM in the original basis is actually smaller than the evidence of most MCM with same rank in the \mathbf{b}^* basis, which highlights the advantage of choosing the best IM as a basis for searching for the best MCM (see Fig. S2 for mode details). Finally, note that the best MCM identified by our algorithm has $K_{\text{MCM}} = (2^5 - 1) + (3^3 - 1) + 1 = 39$ operators, which is smaller than the number of parameters $K_{\text{pair}} = 9 \times 10/2 = 45$ of a fully connected pairwise model.

Boolean description of a binary dataset

Next, we tested our approach on an artificial dataset of $n = 9$ variables and $N = 10^5$ datapoints that we generated by sampling randomly three different states, S_1 , S_2 and S_3 , with different probabilities, respectively $p_1 = 0.2$, $p_2 = 0.3$ and $p_3 = 0.5$ (see Fig. 5.a). There were no additional patterns or sources of noise in the data. The size of the system ($n = 9$) was chosen sufficiently small to easily perform the exhaustive search described in the previous section. The factor graph of the best MCM found for this dataset is shown in Fig. 5.b. It is composed of 8 ICCs, 7 of which are based on a single operator (green triangles).

Once it is fitted, this MCM can be used as a generative model. As discussed in Methods 1.1, fitting an MCM does not require fitting the vector of parameters \mathbf{g} , because one can directly fit the probability of the states described by each ICC. Indeed, for an ICC \mathcal{M}_a , the likelihood is maximized when the probability of occurrence of the states of \mathbf{b}_a in the model is equal to their probability of occurrence in the data (see Eq. (9) and Methods 1.1). We thus obtain that all the single-operator ICCs (green triangles in Fig. 5.b) are associated to statement that are true with probability 1 over the entire dataset, i.e. they are associated to independent tautologies of the data. For instance, in this dataset, the operator $\phi_1 = s_8 s_9$ is equal to 1 with probability 1 and the operator $\phi_5 = s_3 s_9$ is equal to -1 with probability 1, i.e., the two statements $\phi_1 = 1$ and $\phi_5 = -1$ are true over the entire dataset. After taking into account the 7 independent tautologies, we are left with only four states that could be generated by the best MCM (see Fig. 5.c), each of them corresponding to a different value of the basis elements $\mathbf{b}_a = (\phi_8, \phi_9)$ of the last ICC (orange triangle). Fitting the probabilities of occurrence of \mathbf{b}_a on the data, we obtained that $P(\phi_8 = -1, \phi_9 = 1) = 0.2$, $P(1, -1) = 0.3$, $P(1, 1) = 0.5$ and, by normalization, $P(-1, -1) = 0$ (there are only three independent probabilities). This finally provides a full description of the rules used to generate the data. In this case, we observe that the best MCM provides the shortest complete description of the data in terms of spin models. Note that because each spin operator is associated to an elementary

⁶For $n = 9$, the program in [20] takes less than a second to find the best MCM on a simple laptop.

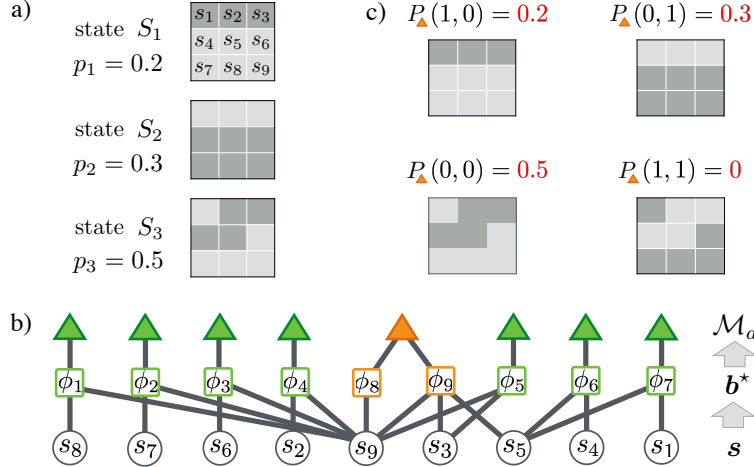


Figure 5: **Analysis of a simple artificial dataset.** **a)** We generated a dataset composed of three different states (S_1 , S_2 and S_3) each sampled with a different probability (respectively p_1 , p_2 and p_3). Dark pixels correspond to the spin state $s_i = -1$, and light pixels to $s_i = +1$. **b)** Factor graph of the best MCM found for this dataset. **c)** Once it is fitted, the best MCM can generate four different states. Three of them are the original states and are sampled with the same probability than their occurrence in the original dataset, the last one is sampled with probability 0.

boolean functions⁷, the best MCM therefore also provides a complete decomposition of the data in terms of such boolean functions. each associated with a parameter that is the probability that this function takes value 1 over the dataset (7 of which being just probability 1 or 0).

MC selection, heuristics for large systems

When n is large and exhaustive search is unfeasible, we propose the following heuristics. In order to find the best IM \mathbf{b}^* , we start from an initial basis \mathbf{b} (e.g., $\mathbf{b} = \mathbf{s}$), and we build all interactions up to a chosen order k . Among these interactions, we identify the set \mathbf{b}' of n independent operators that is maximally biased, and replace \mathbf{b} by \mathbf{b}' . We repeat this procedure until we find $\mathbf{b}' = \mathbf{b}$. This final basis is our best choice for the IM \mathbf{b}^* . Although the exploration of the space of IM is limited by the choice of k , the iteration of this procedure is able, in principle, to explore the space of operators to any order.

Next, we apply an hierarchical merging procedure to find the optimal MCM. We start from the IM based on the basis operators \mathbf{b}^* identified above, which is an MCM with n ICC of rank $r_a = 1$. We merge two ICCs \mathcal{M}_a and $\mathcal{M}_{a'}$ in all possible ways. Among these combinations, we identify the pair that yields a maximal increase of the evidence in Eq. (8) and merge the corresponding ICCs. This procedure generates an approximation of the MCM that achieves a maximal value of the evidence along the hierarchical merging process, as the number of ICCs varies from n to 1.

Big Five Personality Test [27]

We applied this algorithm to several datasets, performing the iterative search for the best basis at the $k = 4^{\text{th}}$ order. Figure 6 reports the resulting MCM for the Big Five Personality Test [27]. The test consists of $n = 50$ questions designed to probe the personality of individuals along five different dimensions, that have been suggested as the main traits describing personality. These traits are extraversion, neuroticism, agreeableness, conscientiousness and openness to experience. Each trait is evaluated from the answers to ten questions, on a scale of one (disagree) to five (agree), that can be either positively or negatively associated with the trait⁸. Data on $N = 1\,013\,558$ samples were taken from Ref. [28], to which we refer for more details. We converted each answer in binary format, depending on whether it was positively or negatively associated with the trait with respect to the average score across the whole sample. For this dataset, inference within the family of MCMs can reveal whether or not the data confirms the hypothesis that these questions probe the respondent's personality along five dimensions, and how these dimensions are associated with the

⁷A spin state can be re-written as $s_i = (-1)^{x_i}$ where $x_i \in \{-1, +1\}$. Thus the spin operator $\phi^\mu(\mathbf{s}) = \prod_{i \in \mu} s_i$ corresponds to the boolean function $\phi^\mu(\mathbf{x}) = \bigoplus_{i \in \mu} x_i$, where \bigoplus is the XOR operator, and $\phi^\mu(\mathbf{s}) = (-1)^{\phi^\mu(\mathbf{x})}$.

⁸For example, agreeableness is probed by questions such as ‘‘I sympathise with others’ feelings’’ or ‘‘I insult people’’.

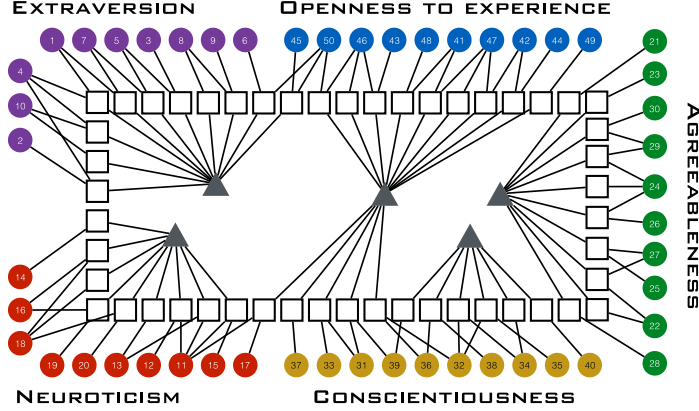


Figure 6: Factor graph representation of the best MCM found with our heuristic algorithm for the Big Five Personality Test dataset.

questions of the test. Our result, obtained with the heuristic algorithm, is shown in Fig. 6 top. Here as well, the best basis \mathbf{b}^* contains exclusively single-body and two-body operators. With the exception of one⁹, all these interactions are confined to questions relative to the same trait. The best MCM we found has five ICCs, each mainly grouping together interactions related to the same trait, apart from one ICC that significantly mixes conscientiousness and openness. The log-evidence of this MCM ($\log E \simeq -2.596 \cdot 10^7$) is however still smaller than the log-evidence of the MCM with 5 ICCs exactly grouping together all the interactions related to the same trait ($\log E \simeq -2.518 \cdot 10^7$). This result shows that this latter MCM is indeed one of the best (see distribution of the log-evidence of MCMs with 5 ICCs in Fig. S3), and overall, this analysis confirms that the questions of the Big Five Personality Test accurately probe the desired five independent traits [27]. Our analysis also found dependencies among the questions within each trait, which could be used to further improve the design or the analysis of the test. Finally, this analysis suggests that a measure based on the log-evidence of MCMs can be used to assess the quality of a personality test.

Modeling the MNIST database [29]

Finally, we performed BMS with MCMs on the MNIST database [29], which is composed of $N = 60000$ images of hand-written digits. In order to reduce the data to a manageable size, given our computational resources¹⁰, we coarse grained it in cells of 2×2 pixels, that were converted into binary values by applying a threshold¹¹. We focus on a central zone of $n = 11 \times 11 = 121$ pixels. Fig. 7.a shows the evidence as a function of the number $A = |\mathcal{A}|$ of ICCs at different stages of the hierarchical merging procedure. A maximum is achieved at $A = 15$. The structure of the inferred MCM at $A = 15$ is rather complex, with several high order interactions, which are grouped in relatively large ICCs (see Fig. 7.b and c).

The aim of this exercise is to test the efficiency of the inferred MCMs in generalization. For this purpose, we sample digits from the maximum likelihood distribution at different values of A . In order to generate a new digit s , we perform the following steps: *i*) we sample a random value of \mathbf{b}_a directly from the data, for each $a \in \mathcal{A}$; *ii*) the sampled state $\mathbf{b}^* = \{\mathbf{b}_a, a \in \mathcal{A}\}$ is then obtained by combining the states of each \mathbf{b}_a ; finally *iii*) we get the sampled digit s in the original basis, by inverting the GT \mathcal{T} that maps s to \mathbf{b}^* and using $s = \mathcal{T}^{-1}(\mathbf{b}^*)$. As shown in Methods 1.3, this last step requires the inversion of an $n \times n$ binary matrix (modulo 2), which needs only to be performed once. Step *i*) exploits the fact the ICC \mathcal{M}_a is complete on \mathbf{b}_a , and therefore, computing \mathbf{b}_a on a randomly drawn digit from the dataset \hat{s} generates values of \mathbf{b}_a that are distributed according to Eq. (9). Hence, a new state of \mathbf{b}^* can be generated in a straightforward manner from A independent draws from the dataset. And therefore, sampling from the likelihood of the inferred MCM is remarkably simple. Notice that, for $A = 1$ this procedure amounts to sampling digits directly from the original dataset. For $A > 1$, sampling generates new patterns, as shown in the inset of Fig. 7 a). Although the sampled images have some structure, their resemblance to digits fades away as A increases.

⁹We found a pairwise interaction between the question ‘‘I’m full of ideas’’, that should probe openness to experience, and ‘‘I have little to say’’, that probes (negatively) extraversion.

¹⁰All calculations were performed on a laptop computer.

¹¹If the sum of the grey levels of the four pixels exceeds 400, the coarse grained pixel is assigned the value one, otherwise it is zero. Our code employs bitwise operations on 16 bytes integers, thus limiting the size of the systems we could handle to $n \leq 128$.

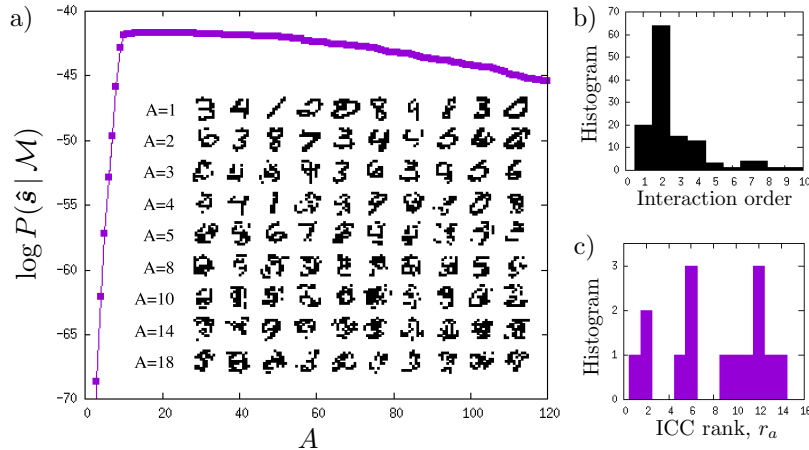


Figure 7: **a)** Evidence of the selected MCM as a function of the number $A = |\mathcal{A}|$ of ICCs during the merging procedure. The maximum is attained at $A = 15$. The inset shows sample digits drawn from the maximum likelihood distribution at different values of A . The top row refers to the original data ($A = 1$). **b)** Histogram of the order of the interactions in the best IM. There is a significant number of interactions that are of order higher than pairwise. **c)** Histogram of the rank r_a (“size”) of the 15 ICCs of the best MCM found with the merging procedure.

Discussion

Finding the model that best describes a dataset within Bayesian model selection is a daunting task. We show that this task is considerably simplified when the selection is restricted to the family of MCMs. These models are simple in terms of their description length complexity, and they are easy to infer. BMS within MCMs probes interaction of arbitrary order and can reveal the presence of high order interactions or confirm that low order interactions are prevalent in a dataset. In addition, MCMs disentangle the structure of statistical dependence into independent components. As such, it can be a useful preprocessing step to divide the inference problem into smaller problems that can be analysed in more detail. Furthermore, this structure provides a notion of locality that could be used in coarse-graining procedures in the context of data renormalisation [30], going beyond pairwise correlations. Finally, the invariance under GTs of the family of MCMs ensures that the inference process is independent of how data is represented¹². This is not true when model selection is restricted to a family of models that is not invariant under GTs, such as the family of pairwise models. In this case, it may be hard to say whether the structure of the inferred model reflects statistical dependencies of the data or the constraints imposed by the considered family of models.

Our approach departs from the literature on graphical model reconstruction [10, 31, 12, 13] in important ways. The latter aims at retrieving a model from a dataset generated from it, by identifying which interactions among a pre-assigned set (e.g. pairwise) are present. Here we do not make any assumptions on the interactions present in the models. Most importantly, we are not interested in reconstructing a specific model from which the data could have been generated. Instead, we aim to find the most likely *simple* model for data, which can inform us on the real structure of dependencies in the data. A critical aspect in graphical model reconstruction is parameter estimation, for which different approximate algorithms have been proposed [14]. We show that there is no need to infer model parameters in order to perform model selection among MCMs, which is a huge computational advantage. Moreover, MCMs can be directly compared on the basis of their evidence, which allows to balance goodness-of-fit and model complexity. In contrast, the model complexity of graphical models is difficult to compute, which calls for adopting regularisation methods [31, 14], which have no clear information theoretical foundation. Finally, the set of models that can be compared in BMS within the family of MCMs is much larger than the number of possible pairwise models usually considered (see Fig. 2).

In summary, this paper offers a novel perspective on statistical inference of high dimensional data, by focusing on simple representations of data. Further extensions beyond binary variables, as well as the development of efficient algorithms to find the MCM with maximal evidence for large systems, are promising avenues of research.

¹²Consider, for a purely illustrative purpose, an idealised problem of inference in a gene regulatory network. Assume that whether gene i is expressed ($s_i = +1$) or not ($s_i = -1$) depends on whether its t_i transcription regulators are bound ($\sigma_{i,a} = +1$) or not ($\sigma_{i,a} = -1$) to the regulator binding region, i.e. that $s_i = f_i(\sigma_{i,1}, \dots, \sigma_{i,t_i})$ is a boolean function of the $\sigma_{i,a}$ ’s. If the relation between s and σ is a GT, then our approach ensures that inference of the gene regulatory network based on a dataset \hat{s} of gene expression should give the same results as inference based on a dataset $\hat{\sigma}$ of binding on regulatory regions.

Materials and Methods

1.1 Maximum Likelihood and Evidence of an ICC

Let us consider an ICC \mathcal{M}_a with rank r_a , and a basis $\mathbf{b}_a(\mathbf{s}) = (\phi_1(\mathbf{s}), \dots, \phi_{r_a}(\mathbf{s}))$ of \mathcal{M}_a . The probability distribution of the states of the system under \mathcal{M}_a can be re-written in the basis of operators \mathbf{b}_a as:

$$P(\mathbf{s} | \mathbf{g}, \mathcal{M}_a) = \frac{1}{2^{(n-r_a)}} q(\mathbf{b}_a(\mathbf{s})), \quad (10)$$

where $q(\mathbf{b}_a) = P(\mathbf{b}_a | \mathbf{g}, \mathcal{M}_a)$ is a normalised probability distribution over the states of $\mathbf{b}_a \in \{\pm 1\}^{r_a}$. For an ICC \mathcal{M}_a , there is a bijective map between the $2^{r_a} - 1$ parameters g^μ of \mathcal{M}_a and the $2^{r_a} - 1$ states probabilities $q(\mathbf{b}_a)$ (the last probability being fixed by the normalization). More precisely, the value of the parameters g^μ can be obtained from the states probabilities $q(\mathbf{b}_a)$ by taking the logarithm of Eq. (10), multiplying by $\phi^\mu(\mathbf{s})$ and summing over all the states of \mathbf{s} . Finally using the orthogonality relation between operators, one finds that for all interaction $\mu \in \mathcal{M}_a$:

$$g^\mu = \frac{1}{2^n} \sum_{\mathbf{s}} \phi^\mu(\mathbf{s}) \log q(\mathbf{b}_a(\mathbf{s})), \quad \forall \mu \in \mathcal{M}_a. \quad (11)$$

Note that for $\mu \notin \mathcal{M}_a$ this equation yields $g^\mu = 0$, because the function $q(\mathbf{b}_a(\mathbf{s}))$ is expressed solely in terms of the operators $\mu \in \mathcal{M}_a$. Statistical inference of ICCs, and therefore of MCMs, is more easily done in the q -representation, i.e. in terms of the parameters $q(\mathbf{b}_a)$. The result can then be re-written in the original spin model representation using Eq. (11).

Using Eq. (10), the likelihood function of an ICC \mathcal{M}_a for a dataset $\hat{\mathbf{s}}$ can be written as:

$$P(\hat{\mathbf{s}} | \mathbf{g}, \mathcal{M}_a) = \frac{1}{2^{N(n-r_a)}} \prod_{\mathbf{b}_a} q(\mathbf{b}_a)^{k_{\mathbf{b}_a}}, \quad (12)$$

where the product is over all possible 2^{r_a} values of \mathbf{b}_a , and where $k_{\mathbf{b}_a}$ is the number of times the basis operators take a given value \mathbf{b}_a over the entire dataset. Thanks to the bijection between the $2^{r_a} - 1$ parameters \mathbf{g} and the $2^{r_a} - 1$ parameters $q(\mathbf{b}_a)$, the maximum likelihood can be obtained by maximizing Eq. (12) directly over the parameters $q(\mathbf{b}_a)$. From this maximization, one finds that the maximum likelihood estimate of q is:

$$\hat{q}(\mathbf{b}_a) = \frac{k_{\mathbf{b}_a}}{N}. \quad (13)$$

Combined with Eq. (7) and Eq. (12), this leads to the result in Eq. (9) for the maximum likelihood of an MCM.

The calculation of the evidence of an ICC is likewise straightforward. We first exploit the invariance of Jeffreys prior under reparametrization [17], which takes the following form in the q -representation:

$$P_0(\mathbf{q} | \mathcal{M}_a) = \frac{\Gamma(2^{r_a-1})}{\pi^{2^{r_a-1}}} \prod_{\mathbf{b}_a} \sqrt{q(\mathbf{b}_a)} \delta\left(\sum_{\mathbf{b}_a} q(\mathbf{b}_a) - 1\right), \quad (14)$$

where we denote by \mathbf{q} the vector of 2^{r_a} probabilities $q(\mathbf{b}_a)$. Combined with the expression of the likelihood in Eq. (12), this yields:

$$P(\hat{\mathbf{s}} | \mathcal{M}_a) = \int d\mathbf{g} P(\hat{\mathbf{s}} | \mathbf{g}, \mathcal{M}_a) P_0(\mathbf{g} | \mathcal{M}_a) \quad (15)$$

$$= \frac{1}{2^{N(n-r_a)}} \frac{\Gamma(2^{r_a-1})}{\pi^{2^{r_a-1}}} \int_0^1 d\mathbf{q} \prod_{\mathbf{b}_a} q(\mathbf{b}_a)^{k_{\mathbf{b}_a} + \frac{1}{2}} \delta\left(\sum_{\mathbf{b}_a} q(\mathbf{b}_a) - 1\right) \quad (16)$$

$$= \frac{1}{2^{N(n-r_a)}} \frac{\Gamma(2^{r_a-1})}{\Gamma(N + 2^{r_a-1})} \prod_{\mathbf{b}_a} \frac{\Gamma(k_{\mathbf{b}_a} + \frac{1}{2})}{\sqrt{\pi}}. \quad (17)$$

This calculation easily generalizes to MCMs, in which the components \mathcal{M}_a are associated to independent basis elements \mathbf{b}_a . We recall that the likelihood, the prior and the evidence of an MCM factorizes over its independent components, using Eq. (7). This finally leads to the expression of the evidence of an MCM given Eq. (8).

1.2 Search for the best IM

An independent model (IM) is an MCM in which all the components \mathcal{M}_a only contain a single operator ($r_a = 1$ for all $a \in \mathcal{A}$). Let us focus on the case where the number of components $|\mathcal{A}|$ is equal to the number of spins n . Model selection among these models only requires to compare their likelihood, because they all have the same complexity terms. The maximum log-likelihood of an independent model takes the simple form:

$$\log P(\hat{\mathbf{s}} | \hat{\mathbf{g}}, \mathcal{M}) = -N \sum_{a=1}^n H[m_a] \quad (18)$$

where the sum is over the n components, and where

$$H[m] = -\frac{1+m}{2} \log \frac{1+m}{2} - \frac{1-m}{2} \log \frac{1-m}{2} \quad (19)$$

and

$$m_a = \frac{1}{N} \sum_{i=1}^N b_a(\mathbf{s}^{(i)}) \quad (20)$$

is the bias of operator b_a . The function $H[m]$ is maximal for $m = 0$ and it achieves its minimal value $H[m] = 0$ when $m = 1$ or $m = -1$. This implies that the most likely independent model is given by the most biased set \mathbf{b} of independent operators.

The algorithm to find these operators is a recursive one: Let b_1 be the most biased operator ϕ^μ , i.e. the one with the largest average value of $|\phi^\mu|$ in the dataset. Add the next most biased operator b_2 . The third operator b_3 is the most biased one, excluding the operator $b_1 b_2$, which is not independent from the previous two. Proceeding in this way, at step r , let $\mathbf{b}_{<r} = (b_1, \dots, b_{r-1})$ be the set of independent operators already identified. This divides the set of all operators in the subset $\mathcal{I}_{<r}(\mathbf{b}_{<r})$ that are combinations of the operators $\mathbf{b}_{<r}$ and the set $\mathcal{I}_{\geq r}(\mathbf{b}_{<r})$ of operators that are independent of $\mathbf{b}_{<r}$. Choose the most biased operator $b_r \in \mathcal{I}_{\geq r}(\mathbf{b}_{<r})$ and add it to the set $\mathbf{b}_{<r}$. This gives $\mathbf{b}_{<r+1} = (\mathbf{b}_{<r}, b_r)$. Iterate until $r = n$.

In order to show that this procedure generates the best independent model, consider replacing b_r with any other operator b . Since \mathbf{b} is a complete basis for all operators, b has to be expressed in terms of them. With some abuse of notation, we write this as

$$b = \prod_{a \in \mathbf{b}} b_a = b_r b_{b-r}. \quad (21)$$

The second relation expresses the fact that the operator b_r necessarily appears in this product, because the new basis \mathbf{b}' with b_r replaced by b , has to be complete. In Eq. (21) b_{b-r} stands for the product of the other operators in \mathbf{b} excluding b_r , that generate b .

It follows that the bias of the new operator

$$m_b = \frac{1}{N} \sum_{i=1}^N b(\mathbf{s}^{(i)}) = \frac{1}{N} \sum_{i=1}^N b_r(\mathbf{s}^{(i)}) b_{b-r}(\mathbf{s}^{(i)}) \leq m_r. \quad (22)$$

The last inequality derives from the fact that, by construction, b_r is the most biased operator among all those that contain b_r .

1.3 Sampling from an MCM

The probability distribution of a chosen MCM \mathcal{M} at best fit reads:

$$P(\mathbf{s} | \hat{\mathbf{g}}, \mathcal{M}) = \frac{1}{2^{n-r}} \prod_{a \in \mathcal{A}} \frac{k_{\mathbf{b}_a(\mathbf{s})}}{N}, \quad (23)$$

where $k_{\mathbf{b}_a}/N$ are the empirical probabilities of the states of \mathbf{b}_a in the data. To sample a configuration \mathbf{s} from this model, we draw a configuration of \mathbf{b}_a with probability $q(\mathbf{b}_a) = k_{\mathbf{b}_a}/N$ for each ICC \mathcal{M}_a . This can be done by sampling directly from the empirical distribution $q(\mathbf{b}_a)$, or by drawing uniformly a configuration \mathbf{s}^a from the data and then computing the transformation $\mathbf{b}_a(\mathbf{s}^a)$ (Eq. (23) ensures that this procedure produces a sample value of \mathbf{b}_a with the correct distribution). We then concatenate the \mathbf{b}_a vectors to obtain a value of the state vector $\mathbf{b} = \cup_{a \in \mathcal{A}} \mathbf{b}_a$. The last $(n-r)$ spin states, which are not modeled by \mathcal{M} , are randomly sampled with probability 1/2 to be +1 or -1, and placed in the $(n-r)$ -dimensional vector $\bar{\mathbf{b}}$. Completing the basis $\mathbf{b}(\mathbf{s})$ of \mathcal{M} with $(n-r)$ independent operators forms

a basis of the whole n -dimensional spin space, which defines a GT \mathcal{T} . Finally, we perform an inverse GT to obtain a sampled value of $\mathbf{s} = \mathcal{T}^{-1}(\mathbf{b} \cup \bar{\mathbf{b}})$.

This last part involves the inversion of an $n \times n$ binary matrix modulo 2. Indeed, spins can be represented as $s_i = (-1)^{x_i}$, with $x_i = 0$ or 1. A spin configuration $\mathbf{s} = (s_1, \dots, s_n)$ then corresponds to a string of n bits $\mathbf{x} = (x_1, \dots, x_n)$. A basis configuration $\mathbf{b} = (b_1, \dots, b_n)$ can also be represented in terms of a bit string $\mathbf{y} = (y_1, \dots, y_n)$, with $b_j = (-1)^{y_j}$. Then the GT $\mathbf{b}(\mathbf{s})$ corresponds to the matrix product:

$$\mathbf{y} = \mathbf{x} \cdot \hat{\mathbf{T}}, \quad (24)$$

where \mathbf{x} and \mathbf{y} are row vectors, and where summations are performed modulo 2. Here, the elements of the matrix $\hat{\mathbf{T}}$ are such that $T_{i,j} = 1$ if the basis operator b_j contains spin s_i , and $T_{i,j} = 0$ otherwise. This way, one gets $y_j = 1$ if and only if the number of negative spins that contribute to b_j in configuration \mathbf{s} is odd. Therefore, to obtain the value of \mathbf{s} that corresponds to a value of the basis \mathbf{b} , we need to invert the matrix $\hat{\mathbf{T}}$ and compute $\mathbf{x} = \mathbf{y} \cdot \hat{\mathbf{T}}^{-1}$. This inversion step can be done once, by Gaussian elimination. In summary, sampling from the best MCM requires drawing A independent configurations $\mathbf{s}^{(i_a)}$ from the dataset $\hat{\mathbf{s}}$ and a matrix multiplication, modulo 2.

Acknowledgements

We gratefully acknowledge Edward D. Lee and William Bialek for sharing the data of [8]. We are grateful to the authors of Ref. [32] for sharing their data. We are grateful to Iacopo Mastromatteo, Vijay Balasubramanian, and Yasser Roudi for insightful discussions.

Supplementary Materials

1.4 Background: useful results and definitions

This section provides a summary of definitions and results from Ref. [6] that are used in the main text and in this document. We refer the reader to Ref. [6] for comments and proofs of the results recalled in this section.

Spin operator and spin model

A *spin model* is a probabilistic model that describes the state of a system of binary variables, called *spins*. The model assumes the existence of interactions between the spins that constrain the states accessible to the system. As no spatial organisation is assumed, interactions can be of arbitrary order and of arbitrary range. To mathematically define a spin model, each interaction of the model is associated with a *spin operators*.

More precisely, consider a system of n spin variables, $\mathbf{s} = (s_1, \dots, s_n)$, that take random binary values $s_i = \pm 1$. A *spin operator* $\phi^\mu(\mathbf{s})$ associated with an interaction labeled by μ is defined as the product of the spin s_i involved in the interaction:

$$\phi^\mu(\mathbf{s}) = \prod_{i \in \mu} s_i. \quad (25)$$

In practice, μ can be taken as an n -dimensional binary vector encoding which spin is involved in the interaction (i.e., its i -th element $\mu_i = 1$ if spin s_i is included in the interaction, and $\mu_i = 0$ otherwise). The product in Eq. (25) is then over all the indices i such that the i -th element of μ is 1. The number of spin operators is therefore the number of non-null such binary vector μ , which is $2^n - 1$. With the addition of the identity operator, $\phi^0(\mathbf{s}) = 1$ for all \mathbf{s} , the set of all operators $\{\phi^\mu\}$ forms a group, in the sense that the product $\phi^\mu \phi^\nu = \phi^{\mu \oplus \nu}$ of any two operators is an operator¹³. Notice that the square of any spin variable s_i and of any operator is equal to one. The set of operators forms also a complete and orthogonal basis for all functions of n binary variables, as

$$\sum_{\mathbf{s}} \phi^\mu(\mathbf{s}) \phi^\nu(\mathbf{s}) = 2^n \delta_{\mu,\nu} \quad \text{and} \quad \sum_{\mu=0}^{2^n-1} \phi^\mu(\mathbf{s}) \phi^\mu(\mathbf{s}') = 2^n \delta_{\mathbf{s},\mathbf{s}'}. \quad (26)$$

Hence any function $F(\mathbf{s}) = \sum_{\mu \geq 0} f^\mu \phi^\mu(\mathbf{s})$ defined on the spin configurations can be represented as a linear combination of spin operators, with coefficients given by $f^\mu = 2^{-(n-1)} \sum_{\mathbf{s}} \phi^\mu(\mathbf{s}) F(\mathbf{s})$. These completeness relations hold also on the sub-space defined by a subset of the spins, or by a set of independent operators.

¹³The operator \oplus is the bitwise XOR Boolean operator applied to the two binary vectors μ and ν .

A *spin model* is a maximum entropy model, whose Hamiltonian is a linear combination of the elements of a set \mathcal{M} of spin operators. The probability distribution over the spin variables \mathbf{s} under a spin model \mathcal{M} is therefore:

$$P(\mathbf{s} | \mathbf{g}, \mathcal{M}) = \frac{1}{Z_{\mathcal{M}}(\mathbf{g})} \exp\left(\sum_{\mu \in \mathcal{M}} g_{\mu} \phi^{\mu}(\mathbf{s})\right), \quad \text{with} \quad Z_{\mathcal{M}}(\mathbf{g}) = \sum_{\mathbf{s}} \exp\left(\sum_{\mu \in \mathcal{M}} g_{\mu} \phi^{\mu}(\mathbf{s})\right), \quad (27)$$

where $\mathbf{g} = \{g_{\mu}, \mu \in \mathcal{M}\}$ is a vector of real parameters and where the partition function $Z_{\mathcal{M}}(\mathbf{g})$ ensures normalisation. Each parameter g_{μ} modulates the strength of the interaction associated with the operator $\phi^{\mu}(\mathbf{s})$. In an n -spin system, there are $2^n - 1$ different spin operators, hence there are $2^{2^n - 1}$ different spin models that can be constructed. Each model is identified with the set \mathcal{M} of spin operators that it contains.

Set of independent operators

The operators ϕ^{μ} in a set \mathcal{I} are said *independent* if none of the operators of the set can be obtained as a product of any subset of other operators of the set \mathcal{I} . For example, the sets $\{s_1, s_2, s_3\}$ and $\{s_1, s_1 s_2, s_1 s_2 s_3\}$ are two examples of such set, whereas $\{s_1, s_2, s_1 s_2\}$ is a counter-example, because any operator in this set equals the product of the two other operators. In an n -spin system, the set of the n spin variables $\mathcal{I}_s = \{s_1, \dots, s_n\}$ is set of independent operators. All the operators of the system are generated as products of the n basis spin elements (s_1, \dots, s_n) . Since there is no other independent operator, a set of independent operators can have at maximum n elements.

Gauge transformation

If $\mathcal{I} = \{\phi_1(\mathbf{s}), \dots, \phi_n(\mathbf{s})\}$ is a set of n independent operators, the transformation $\mathbf{s} \rightarrow \mathbf{s}'$ where $s'_i(\mathbf{s}) = \phi_i(\mathbf{s})$ establishes a one to one mapping between the set of states onto itself. This also establishes a bijection of the set of operators onto itself and of the set of models. Following Ref. [6], we call this a *gauge transformations* (GTs). A GT can be thought of as a change of basis from the original spin representation to a new one. Figure 3 of the main text shows some examples of gauge transformations.

Ref. [6] shows that a GT leaves the partition function $Z_{\mathcal{M}}(\mathbf{g})$ of a model invariant up to permutation of its parameters. Likewise, the Fisher Information matrix

$$I_{\mu, \nu}(\mathbf{g}) = \partial_{g_{\mu}} \partial_{g_{\nu}} \log Z(\mathbf{g}) \quad (28)$$

enjoys the same invariance property. This shows that the model complexity

$$c_{\mathcal{M}} = \int d\mathbf{g} \sqrt{\det I(\mathbf{g})} \quad (29)$$

is invariant under GTs. This allows to classify all models into equivalence classes, characterised by the same complexity $c_{\mathcal{M}}$ (see Ref. [6]).

Independent Models

An *Independent Model* (IM) is a spin model defined by a set of r independent spin operators, $\mathcal{M}_{ind} = \{\phi_1, \dots, \phi_r\}$, where necessarily $r \leq n$. A model with r different single-body interactions $\mathcal{M}_{ind} = \{s_{i_1}, \dots, s_{i_r}\}$ is a straightforward example of an independent spin model. All the IM with r interactions can be obtained by gauge transformations of this model. Among all models with r operators, independent models achieve the maximal value of the complexity, which is given by $r \log \pi$ [6].

Independent Complete Component Models

An *Independent Complete Component* (ICC) model \mathcal{M} is such that for any two operators of \mathcal{M} , $\mu, \nu \in \mathcal{M}$, the product operator $\mu \oplus \nu$ is also an operator of \mathcal{M} . An ICC model has $2^r - 1$ operators, where the rank r is the maximal number of independent operators in \mathcal{M} . In other words, an ICC is a model with all the $2^r - 1$ operators generated by a basis of r independent operators, where $r \leq n$. The ICC model with $r = n$ is called the complete model. A GT transforms an ICC model into another ICC model (see Fig. 3 for examples), which therefore has the same complexity.

Minimally Complex Models

A MCM is a model composed of independent complete components (ICC):

$$\mathcal{M} = \bigcup_{a \in \mathcal{A}} \mathcal{M}_a, \quad (30)$$

where each \mathcal{M}_a is an ICC with rank r_a , and $\mathcal{M}_a \cap \mathcal{M}_{a'} = \emptyset$ for all $a \neq a' \in \mathcal{A}$. A GT maps the family of MCMs into itself, preserving the list of ranks r_a of each ICC.

1.5 Enumeration

Number of independent models

All IM with r interactions can be obtained by gauge transformations of the model $\mathcal{I} = \{s_1, \dots, s_r\}$. Therefore their number equals the number of GTs that transforms this model into different ones, and it is given by:

$$\mathcal{N}_{ind}(n, r) = \frac{1}{r!} \prod_{i=0}^{r-1} (2^n - 2^i). \quad (31)$$

This corresponds to the number of ways of choosing r independent operators in the set of all possible $2^n - 1$ operators, divided by the number of possible permutations of these r elements. The first operator can be chosen in $2^n - 1$ ways. After choosing i independent operators, the $(i+1)^{\text{st}}$ operator can be chosen among $2^n - 2^i$ ones, because 2^i operators are dependent on the first i operators. For large values of n , the number of IM of rank r grows as $2^{nr}/r!$. Summing over all possible values of r (from $r = 0$ to n), we evaluate that the total number of independent models grows roughly as 2^{n^2} (see Fig. 2 of the main text), which is faster than the number of pairwise models in the original basis $\sim 2^{n(n+1)/2}$.

Number of Independent Complete Components of rank r

In an n -spin system, all the ICCs of a given rank r can be obtained by taking all possible GTs of any chosen ICC \mathcal{M} of rank r . As the GTs that involve only the operators in \mathcal{M} leaves \mathcal{M} invariant, the number of ICCs is therefore given by

$$\mathcal{N}_{ICC}(n, r) = \prod_{i=0}^{r-1} \frac{2^n - 2^i}{2^r - 2^i}. \quad (32)$$

Here the numerator $\prod_{i=0}^{r-1} (2^n - 2^i)$ counts the number of ways of choosing the r basis operators of the ICC. The denominator $\prod_{i=0}^{r-1} (2^r - 2^i)$ counts the number of GT that transforms the basis of the ICC while leaving \mathcal{M} invariant. The total number of models with a single ICC in an n -spin system is obtained by summing Eq. (32) over all possible values of r ($r = 0$ to n) and is displayed in Fig. 2 of the main text (see curve labelled ‘‘SCM’’).

Number of Minimally Complex Models

For an MCM on n spins with m_{r_a} ICCs of same rank r_a (for all r_a from 1 to n), one can combined the two previous arguments and get:

$$\mathcal{N}_{MCM}(n, \{m_{r_a}\}) = \frac{\prod_{i=0}^{r-1} (2^n - 2^i)}{\prod_{r_a=1}^n m_{r_a}! \left[\prod_{i=0}^{r_a-1} (2^{r_a} - 2^i) \right]^{m_{r_a}}} \quad (33)$$

where the factor $1/m_{r_a}!$ accounts for permutations among ICC of the same size. In order to count the total number of MCMs with n spins (as shown in Fig. 2 of the main text), it is necessary to sum over all the classes of MCMs with different degeneracies m_{r_a} . The number of classes with different degeneracy corresponds to the number of partitions of the rank r of the MCM in the form $r = \sum_{r_a} r_a m_{r_a}$, and summing over all $r \leq n$. For instance, $r = 8$ admits 22 partitions which are:

$$\begin{aligned} &8, 71, 62, 611, 53, 521, 5111, 44, 431, 422, 4211, 41111, 332, 3311, \\ &3221, 32111, 311111, 2222, 22211, 221111, 2111111, 11111111. \end{aligned} \quad (34)$$

The partition ‘‘8’’ corresponds to the class of MCMs that contains only one single ICC with rank $r = 8$. The partition ‘‘422’’ is the class of MCMs formed of three ICC models, with $m_{r_a} = 0$ except for $m_2 = 2$ and $m_4 = 1$.

Number of Minimally Complex Models with the same preferred basis

For a given choice of n basis operators, the number of MCMs of rank $r = n$ that admits that basis as a preferred basis is given by the number of possible partitions of this set of n basis elements, which is given by the Bell number B_n . Ref. [21] gives an upper-bound for the Bell number, $B_n < \left(\frac{0.792n}{\ln(n+1)}\right)^n$. The number of MCM* (indicated in Fig. 2 of

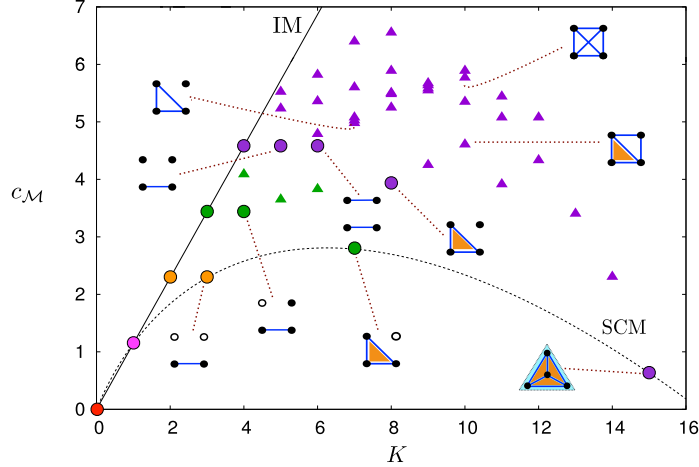


Figure 8: (colors online) **Complexity $c_{\mathcal{M}}$ of all spin models with $n = 4$ spins** as a function of the number of parameters K in the model. Adaptation of Fig. 4 from Ref. [6], where we marked with a circle the classes of MCM. Models of the same class have the same complexity and are represented by either a triangle or a circle (see Ref. [6] for more details). Model representants of some of the classes are displayed using the same diagrammatic notation as in Fig. 1 of the main text. The complexity value of any model lies between two limit lines: one corresponds to the complexity of IM (solid line), the other to the complexity of SCM (dashed line). The colors indicated the number r of independent variables in the model (rank): red for 0, pink for 1, green for 3 and violet for 4. Among all models with same number K of parameters and same rank r , MCMs are the simplest.

the main text) corresponds the total number of MCMs that share the same preferred basis, i.e. the MCMs of any rank from $r = 0$ to $r = n$. This number is given by:

$$\mathcal{N}_{MCM^*}(n) = \sum_{r=0}^n \binom{n}{r} B_r. \quad (35)$$

For example, for $n = 9$ there are 115975 MCMs in total that shares the same preferred basis (i.e., MCM*), 21147 of them have a rank $r = 9$.

References

- [1] George EP Box. Science and statistics. *Journal of the American Statistical Association*, 71(356):791–799, 1976.
- [2] Yann LeCun, Yoshua Bengio, and Geoffrey Hinton. Deep learning. *nature*, 521(7553):436–444, 2015.
- [3] Eugene P Wigner. The unreasonable effectiveness of mathematics in the natural sciences. In *Mathematics and Science*, pages 291–306. World Scientific, 1990.
- [4] Peter D Grünwald and Abhijit Grunwald. *The minimum description length principle*. MIT press, 2007.
- [5] In Jae Myung, Vijay Balasubramanian, and Mark A Pitt. Counting probability distributions: Differential geometry and model selection. *Proceedings of the National Academy of Sciences*, 97(21):11170–11175, 2000.
- [6] Alberto Beretta, Claudia Battistin, Clélia De Mulatier, Iacopo Mastromatteo, and Matteo Marsili. The stochastic complexity of spin models: Are pairwise models really simple? *Entropy*, 20(10):739, 2018.
- [7] Elad Schneidman, Michael J Berry II, Ronen Segev, and William Bialek. Weak pairwise correlations imply strongly correlated network states in a neural population. *Nature*, 440(7087):1007, 2006.
- [8] Cristina Savin and Gašper Tkačik. Maximum entropy models as a tool for building precise neural controls. *Current opinion in neurobiology*, 46:120–126, 2017.
- [9] Edward D Lee, Chase P Broedersz, and William Bialek. Statistical mechanics of the us supreme court. *Journal of Statistical Physics*, 160(2):275–301, 2015.
- [10] Andrea Montanari and Jose A Pereira. Which graphical models are difficult to learn? In *Advances in Neural Information Processing Systems*, pages 1303–1311, 2009.

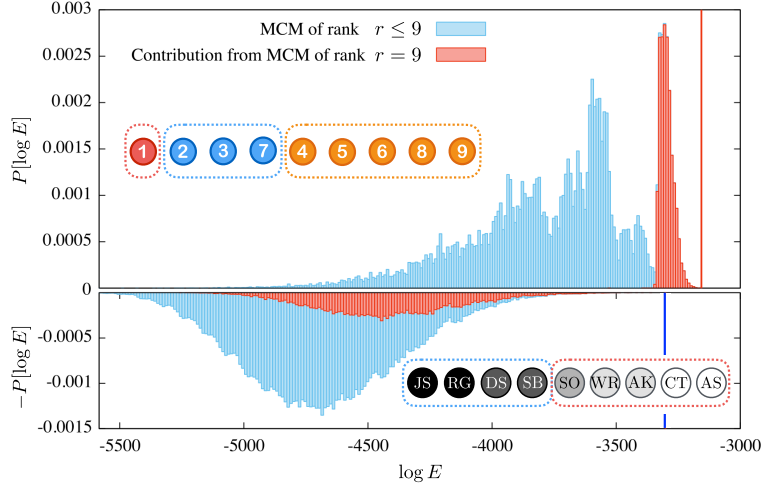


Figure 9: (colors online) **Distribution of the log-evidence of MCMs for the US Supreme court data:** for all the MCMs that admits the best IM \mathbf{b}^* as a preferred basis (top graph, in light blue) and for all the MCMs that admits the original basis of the data as a preferred basis (bottom graph, in light blue). The best MCMs overall is based on \mathbf{b}^* and is shown on the top graph; it has three ICCs, each highlighted by a dotted red, blue or orange square, and has a log-evidence of $\log E \simeq -3327$ (indicated by the vertical red line on the top graph). The best MCM based on the original basis of the justices is shown on the bottom graph; it has two ICCs, each highlighted by a dotted blue or red square and a log-evidence of $\log E \simeq -5258$ (indicated by the vertical blue line on the bottom graph). In both graphs, the distribution in blue corresponds to the distribution of all the MCMs with a chosen preferred basis: with $n = 9$ there are 115975 such models (models of all rank from $r = 0$ to $r = 9$). In both graphs, a part of this distribution has been highlighted in red; it corresponds to the MCMs with rank $r = 9$: with $n = 9$ there are 21147 such models. It is interesting to observe that most MCMs based on the original basis (blue distribution in the bottom graph) have a significantly lower log-evidence than the MCMs of rank $r = 9$ based on the best IM \mathbf{b}^* (red distribution in the top graph).

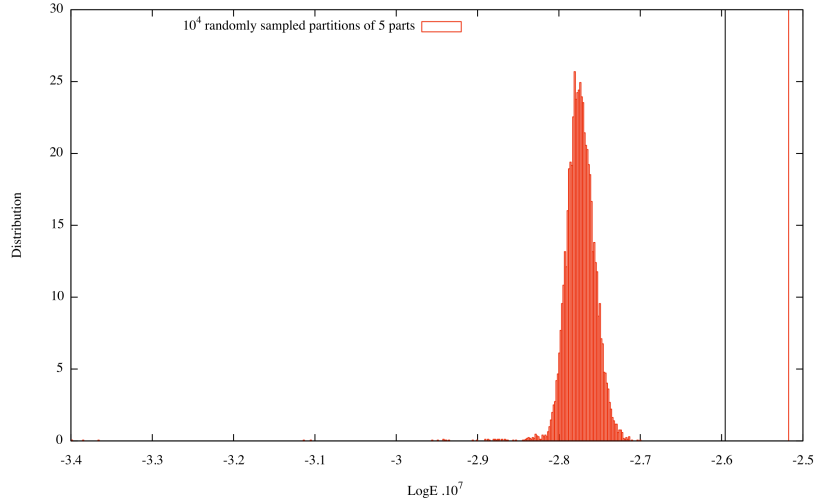


Figure 10: (colors online) **Distribution of the log-evidence of MCMs with 5 ICCs for the Big 5 data in its original basis:** 10^4 partitions of the $n = 50$ questions into $|\mathcal{A}| = 5$ parts (ICCs) were sampled uniformly at random. The log-evidence of the MCM partitioning the questions into the big 5 personalities ($\log E \simeq -2.518 \cdot 10^7$, indicated by a vertical red line) is larger than the best log-evidence found by our heuristic algorithm ($\log E \simeq -2.596 \cdot 10^7$, vertical black line). However, both values of the log-evidence are to the right of the distribution, deep in its tail. There are $\binom{50}{5} = 2\,118\,760$ possible partitions of the 50 questions in 5 parts. Among the 10^4 randomly sampled partitions, the largest evidence found was $\log E \simeq -2.700 \cdot 10^7$ and the lowest evidence was $\log E \simeq -3.399 \cdot 10^7$.

-
- [11] Simona Cocco and Rémi Monasson. Adaptive cluster expansion for the inverse ising problem: convergence, algorithm and tests. *Journal of Statistical Physics*, 147(2):252–314, 2012.
- [12] John P Barton, Eleonora De Leonardis, Alice Coucke, and Simona Cocco. Ace: adaptive cluster expansion for maximum entropy graphical model inference. *Bioinformatics*, 32(20):3089–3097, 2016.
- [13] Marc Vuffray, Sidhant Misra, Andrey Lokhov, and Michael Chertkov. Interaction screening: Efficient and sample-optimal learning of ising models. In *Advances in Neural Information Processing Systems*, pages 2595–2603, 2016.
- [14] H Chau Nguyen, Riccardo Zecchina, and Johannes Berg. Inverse statistical problems: from the inverse ising problem to data science. *Advances in Physics*, 66(3):197–261, 2017.
- [15] Iacopo Mastromatteo. On the typical properties of inverse problems in statistical mechanics. *arXiv preprint arXiv:1311.0190*, 2013.
- [16] John Kruschke. *Doing Bayesian data analysis: A tutorial with R, JAGS, and Stan*. Academic Press, 2014.
- [17] Harold Jeffreys. An invariant form for the prior probability in estimation problems. *Proceedings of the Royal Society of London. Series A. Mathematical and Physical Sciences*, 186(1007):453–461, 1946.
- [18] Jorma Rissanen. Stochastic complexity and modeling. *The annals of statistics*, pages 1080–1100, 1986.
- [19] Jorma J Rissanen. Fisher information and stochastic complexity. *IEEE transactions on information theory*, 42(1):40–47, 1996.
- [20] Clélia de Mulatier. Mincompspin. <https://github.com/clelidm/MinCompSpin>, 2021.
- [21] Daniel Berend and Tamir Tassa. Improved bounds on bell numbers and on moments of sums of random variables. *Probability and Mathematical Statistics*, 30(2):185–205, 2010.
- [22] H.J. Spaeth, L. Epstein, T.W. Ruger, K. Whittington, J.A. Segal, and A.D. Martin. Supreme court database – version 2011 release 3. 2011.
- [23] Luigi Gresele and Matteo Marsili. On maximum entropy and inference. *Entropy*, 19(12), 2017.
- [24] Gideon Ehrlich. Loopless algorithms for generating permutations, combinations, and other combinatorial configurations. *Journal of the ACM (JACM)*, 20(3):500–513, 1973.
- [25] Donald E. Knuth. *The Art of Computer Programming, Volume 4, Combinatorial Algorithms: Part 1*. Addison-Wesley Professional, 2011.
- [26] B. Djokić, M. Miyakawa, S. Sekiguchi, I. Semba, and I. Stojmenović. Short Note: A Fast Iterative Algorithm for Generating Set Partitions. *The Computer Journal*, 32(3):281–282, 01 1989.
- [27] Lewis R Goldberg. The development of markers for the big-five factor structure. *Psychological assessment*, 4(1):26, 1992.
- [28] Bojan Tunguz. Big five personality test. https://openpsychometrics.org/_rawdata/IPIP-FFM-data-8Nov2018.zip. Version 1. Created: 2020-02-17. Accessed: 2020-06-20.
- [29] Yann LeCun, Léon Bottou, Yoshua Bengio, and Patrick Haffner. Gradient-based learning applied to document recognition. *Proceedings of the IEEE*, 86(11):2278–2324, 1998.
- [30] Leenoy Meshulam, Jeffrey L Gauthier, Carlos D Brody, David W Tank, and William Bialek. Coarse graining, fixed points, and scaling in a large population of neurons. *Physical review letters*, 123(17):178103, 2019.
- [31] Pradeep Ravikumar, Martin J Wainwright, John D Lafferty, et al. High-dimensional ising model selection using l_1 -regularized logistic regression. *The Annals of Statistics*, 38(3):1287–1319, 2010.
- [32] Hanne Stensola, Tor Stensola, Trygve Solstad, Kristian Frøland, May-Britt Moser, and Edvard I Moser. The entorhinal grid map is discretized. *Nature*, 492(7427):72–78, 2012.